Determination of a suitable molar absorption coefficient (ε) for lignin analysis of fibrous plants with the CASA method

Antoine Bozek[1,2*], Fabienne Mathis[2], Laurent Guillaumat[3], Jörg Müssig[4], Nathalie Boizot[5,6], Alaa Ismael[1], John Ralph[7,8], Fachuang Lu[7], Richard Sibout[1], Johnny Beaugrand[1*]

[1] UR1268 BIA, INRAE Nantes, BP 71627, 44316 Nantes Cedex 03, France

[2] HEMP-IT-ADN, 6 rue Louis Lumière, 49250 Beaufort en Anjou, France

[3] LAMPA, ENSAM Angers, boulevard du Ronceray, 49100 Angers, France

[4] The Biological Materials Group, Biomimetics, HSB - City University of Applied Sciences, Bremen, Germany, Neustadtswall 30, D-28199 Bremen, Germany

[5] INRAE, ONF, BioForA, UMR 0588, F-45075 Orleans, France

[6] Phenobois Facility, INRAE, 45075 Orleans, France

[7] DOE Great Lakes Bioenergy Research Center, U. Wisconsin, Madison, WI 53726, USA

[8] Department of Biochemistry, U. Wisconsin, Madison, WI 53706, USA

*corresponding authors: antoine.bozek@inrae.fr and johnny.beaugrand@inrae.fr

Abstract

This study evaluates the benchmarking and applicability of the CASA method for the analysis of fibrous plants, such as flax, hemp, and jute. Lignin, a phenolic biopolymer present in plant cell walls, is composed of three primary monomeric units, designated as G, S, and H. Various factors, including genetic variability, influence the relative proportions of these units in plant samples. Recently, the CASA (Cysteine-Assisted Sulfuric Acid) method has been introduced as a rapid method for the quantification of lignin in wood samples. This study aims to establish a suitable molar absorption coefficient (ε, $L \cdot g^{-1} \cdot cm^{-1}$) to adapt the CASA method for use with annual plant fibers. The investigation was motivated by the technical advantages of the CASA method, including higher throughput, lower reaction temperatures, and ecological benefits due to the absence of CMR (carcinogenic, mutagenic, or reprotoxic) substances, as well as the requirement for minimal sample quantities. In this method, lignin solubilization is facilitated by cysteine, an amino acid that enhances the reaction kinetics, allowing for a one-hour incubation period. However, as with any spectrophotometric technique, CASA depends on a molar absorption coefficient (ε) that varies according to the ratio of aromatic units within the polymer. To evaluate the suitability of CASA for quantifying lignin in economically significant plant fibers, we investigate the impact of unit ratios on the accuracy of ε. The results are compared with two widely recognized lignin analytical methods: the Klason method, a gravimetric reference method, and the Acetyl Bromide Soluble Lignin method, the currently most commonly used spectrophotometric approach. The final ε obtained in this study reveals a relative difference in lignin content ranging from -8% to +9% when comparing CASA with the Klason method across different industrial hemp varieties. Based on known G:S ratios in annual fibrous plants, ε can be estimated from our results.

Keywords: Absorption Spectroscopy; Biomass; Composition

Introduction

Annual plants are botanical species that complete their life cycle within a single growing season. The stem fibers of these plants serve a dual purpose – they facilitate nutrient storage [1,2] and support the plant's structural integrity, allowing for an upright growth habit. To achieve this, the fibers must provide stiffness, strength, and elasticity to the stems. The cell walls of these fibers primarily consist of crystalline cellulose, with accompanying components such as amorphous lignin, pectin, and hemicellulose, along with minimal amounts of protein [1,3-6]. Lignin, a hydrophobic phenolic polymer, significantly influences the hydrophobicity and mechanical strength of plant fibers. It is composed of three types of phenylpropanoid units, guaiacyl (G), syringyl (S), and *p*-hydroxyphenyl (H) units that are derived from the hydroxycinnamyl alcohols coniferyl, sinapyl, and *p*-coumaryl alcohols, respectively [7]. The relative proportions of these units can vary widely among different species, plant organs, tissues, and even within specific fractions of the cell wall [1,8].

Among annual plants, industrial hemp (*Cannabis sativa* L.) is a versatile crop cultivated globally, including on marginal lands [9]. The seeds are harvested for food and feed [10] and for lipids production [11]. The stems are also of considerable interest. The central portion, referred to as "hurds" or "shives," [12], provides material reinforcement and is commonly utilized as animal bedding [13,14]. Bast fibers derived from the phloem tissue are employed in the production of composite materials and textiles [15-17]. These fibers can be classified into primary bast fibers, originating from the procambium, and secondary bast fibers, generated by the vascular cambium [2,18]. Primary and secondary fibers exhibit significant differences in dimensions and physical properties [19]. The technical product obtained through mechanical extraction results in long fiber bundles that consist of groups of individual cells or single fibers adhered by components of the middle lamella [1,20,21]. Other annual plants enriched in fibers, such as flax (*Linum usitatissimum* L.) [16], jute (*Corchorus capsularis* L.) [22], nettle (*Urtica dioica* L.) [23], or sisal (*Agave sisalana* PER.) [24] have been investigated for the same purposes. These fibers possess varying mechanical, thermal, as well as end-use properties, and are increasingly recognized as sustainable alternatives to industrially-made fibers [19,25,26] and for producing bio-based composites with desirable properties [27].

In order to predict the properties of natural fibers, research has been conducted to identify correlations between biochemical markers and the intrinsic characteristics of these fibers [4,28-30]. Studies have established connections between the chemical composition of fibers and their hygroscopic or thermal properties [31-33], as well as between lignin content and the mechanical properties of the fibers [19,34,35]. A high Pearson correlation coefficient has been observed in nanoindentation measurements of individual hemp fibers [36]. Lignin also influences fiber yield and post-extraction properties, including variations in tensile or compressive stiffness as measured by Young's modulus [37,38]. It is therefore imperative to accurately measure the composition of the fibers and, by extension, the fiber bundles to optimize the properties of the resultant biobased composite materials.

Several analytical methods are available to quantify the lignin content in samples (Table 1). The standard method is the Klason method [39,40], a gravimetric technique that requires a substantial quantity of material, typically in the gram range. This method involves the hydrolysis of cell wall polysaccharides using sulfuric acid (H_2SO_4) and subsequent gravimetric determination of the insoluble lignin residue. However, the Klason Lignin (KL) method is time-consuming, requiring approximately two days to complete, and necessitates specialized laboratory glassware for each analysis, limiting the number of samples that can be processed simultaneously. Other methods commonly used are the Acetyl Bromide Soluble lignin (ABSL) [41,42] and the Acid Detergent Lignin (ADL) methods [39]. The ABSL method utilizes a spectrophotometric approach wherein the sample is dissolved through acetylation of hydroxyl groups and bromination at benzylic positions. Following this, additional reagents are applied to terminate the reaction, and the absorbance of the hydrolyzed sample is measured at 280 nm [41]. The ADL method was developed by Van Soest [43] as an alternative to Klason Lignin and is optimized specifically for herbaceous samples and typically for ruminant nutrition studies. It also employs H_2SO_4 for hydrolysis, but adds detergent for penetrability and protein removal, and operates under different acid concentration and temperature conditions. The thioglycolic acid (TGA) method estimates lignin content by forming thioethers with the alcohol groups in lignin, producing modified lignins that are soluble under alkaline conditions but insoluble under acidic conditions [44]. Although this method has seen improvements that reduce experimental duration, it still requires a significant sample size of around

80 mg [45]. Moreover, results from the ABSL method are generally considered more accurate than those from TGA [41], although ABSL can suffer from interference from the production of UV-absorbing components, particularly pentoses [46]. Other non-destructive methods, such as Nuclear Magnetic Resonance [47,48], have been investigated. Although NMR provides benefits for structural characterization, it is costly and time-consuming, necessitating specialized procedures for quantitative analysis [48]. Non-destructive methods can be integrated with chemical techniques to gain a deeper understanding of the inherent structure of lignin prior to its dissolution. This approach would allow for the determination of the monomeric composition of lignin and improve the accuracy of subsequent lignin content analyses.

Key parameters, including procedure duration, sample mass requirements, and the generation of ecotoxic byproducts, are crucial for the rapid and systematic quantification of lignin content, particularly in phenotyping campaigns. The recently developed CASA (Cysteine-Assisted Sulfuric Acid, 2021) method addresses many of these technical limitations [49]. Like the ABSL method, CASA is a spectrophotometric technique but utilizes greener chemical reagents and achieves shorter reaction times due to the improved kinetic dissolution of lignins in sulfuric acid facilitated by cysteine, an amino acid. Molar absorption coefficients have been determined for woody samples containing significantly higher lignin levels than fibrous annual plants. Further validation is needed to confirm the suitability of CASA for quantifying lignin in low-lignin-content plant biomass, particularly considering that the proportion of the H monomer is often negligible in trees [49], potentially introducing bias in measurements. We therefore first compared the efficiency of CASA, KL, and ABSL methods using six different annual fibrous plants [flax, hemp, jute, nettle, sisal, and Brachypodium (*Brachypodium distachyon* L.)]. Secondly, we estimated a coefficient of molar absorption to be applied to the hemp material. We end this work by constructing an easy-to-use Abaqus simulation model that links the unit ratios and the molar absorption coefficient of lignin at 283 nm for other sample sources.

Method	Reference	Type	Quantity of sample needed	Procedure duration	Other limits or sensitivity	Supposed ecological impact	Relative difference from Klason
Klason Lignin (KL)	[39]	Gravimetric	High (> 1 g)	Long (>2 days)	Sensitive to proteins	High	/
Thioglycolic Acid Lignin (TGA)	[39]	Absorbance Spectroscopy	Medium (80 mg)	Medium (1 day)	β-O-4 linkage-specific	Medium	-15 %
Acetyl Bromide Soluble Lignin (ABSL)	[41]	Absorbance Spectroscopy	Low (30 mg)	Medium (1 day)	Sensitive to polyphenols (as Tannins) or cell residues	High	+15 %
Acid Detergent Lignin (ADL)	[39]	Gravimetric	High (> 1 g)	Long (>2 days)	Sensitive to proteins	High	±20 %
FTIR	[50]	Spectroscopy	Medium (1 g) and non-destructive	Quick (Half-day)	Not diagnostic or quantitative	Low	N/A
Solution- or Solid-state NMR	[50]	Nuclear Magnetic Resonance	Medium (100 mg) and non-destructive	Quick (Half-day)	Advanced data refining	Low	N/A
Cysteine-Assisted Sulfuric Acid Lignin (CASA)	[49]	Absorbance Spectroscopy	Low (30 mg)	Quick (Half-day)	Tested only on woody samples	Low	**8 % This work**

Table 1. Comparative table of analytical techniques to determine the lignin content in biomass.

Materials and Methods

Chemical products

All the chemical products were supplied by Sigma-Aldrich (Saint Louis, Missouri, USA) except for the sulfuric acid supplied by VWR (Radnor, Pennsylvania, USA).

Plant Materials

Five fiber-enriched plants and five Hemp industrial varieties have been studied in this work (Table 2). The five different industrial varieties of Hemp were cultivated at the Wehnen trial site of the Weser-Ems Chamber of Agriculture in Oldenburg, Germany, under fertilization conditions of 100 kg N/ha and a sowing density of 200 seeds/m². The stems were manually harvested without being subjected to retting, and the leaves were removed by hand. The harvested stems were dried indoors at 18 °C and 45% humidity before being processed. The decortication of hemp stems was carried out with a laboratory breaker [51]. After the decortication, the fiber bundles were refined with a coarse separator [37]. *Brachypodium distachyon* L. was grown in a growth cabinet with 18 h of light at 21 °C as described in [52]

Botanic Species	Origin	Washed (AIR) Not washed (RAW)	Sample name	Reference
Flax (*Linum usitatissimum*)	Bolchoï Variety, 2017, France	AIR	F-AIR	[53]
		RAW	F-RAW	
Hemp (*Cannabis sativa*)	Fedora 17 Variety, France, 2016	AIR	H-AIR	[54]
		RAW	H-RAW	
Jute (*Corchorus capsularis*)	Tossa Variety, Bengal	AIR	J-AIR	[55]
		RAW	J-RAW	
Nettle (*Urtica doica* L.)	Stinging nettle of Roville clone, Doncières, France	AIR	N-AIR	[56]
		RAW	N-RAW	
Brachypodium (*Brachypodium distachyon*)	Bd21-3	AIR	B-AIR	[52]
		RAW	B-RAW	
Sisal (*Agave sisalana*)	Provided by PUC-Rio, Brazil, and cultivated in Valente, Bahia, North of Brazil by the company APAEB	AIR	S-AIR	[56]
		RAW	S-RAW	
Hemp (Fasamo)	Industrial Hemp (details below)	RAW	Fasamo	Details below
Hemp (Fedrina 74)		RAW	Fedrina	
Hemp (USO 31)		RAW	USO	
Hemp (Fedora 17)		RAW	Fedora	
Hemp (Felina 34)		RAW	Felina	

Table 2. Overview of the samples analyzed in this study

Microscopy

Using a scanning electron microscope Phenom Pure G6 Desktop (Thermo-Fischer Scientific, Waltham, MA, USA), images of each sample were captured at an acceleration voltage of 10 kV and a pressure of 1 Pa using the LV detector. Fiber bundles were cut and pasted to carbon pellets before being placed on a sample holder. The various fibrous plant samples were imaged prior to analysis (Fig. 1a and 1b).

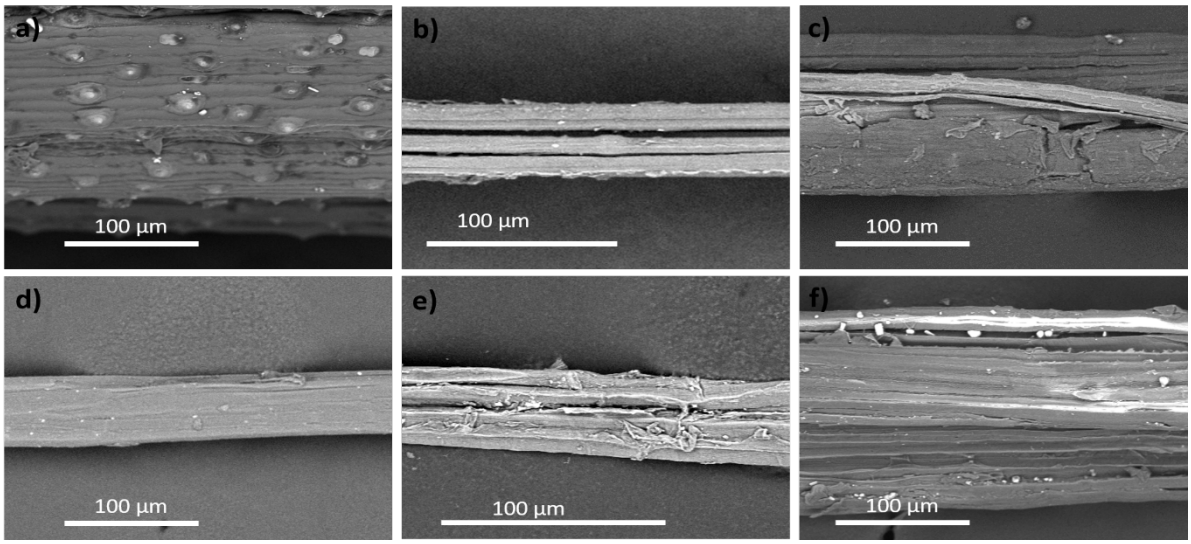

Fig. 1a : SEM images of fiber bundles extracted from samples. a) Brachypodium, b) flax, c) hemp, d) jute, e) nettle, f) sisal.

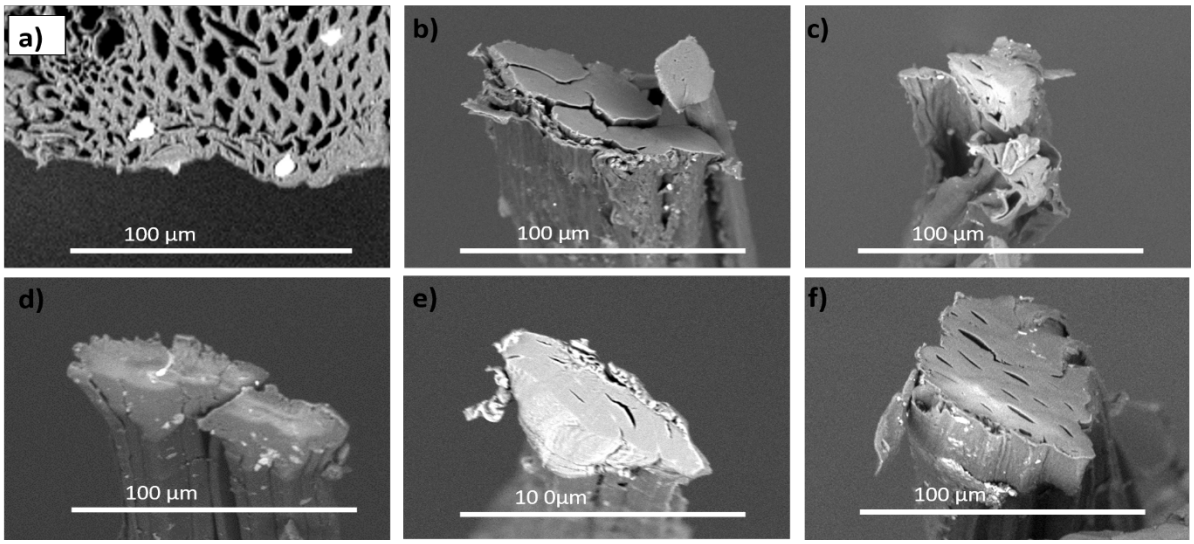

Fig. 1b. SEM images cross-section of fiber bundles extracted from samples. a) Brachypodium, b) flax, c) hemp, d) jute, e) nettle, f) sisal.

1. Sample preparation for lignin analysis

Approximately 600 mg of each raw sample of flax, hemp, jute, sisal and nettle were ground using a freezer/mill 6770 SPEX SamplePrep, a small cryogenic mill (Horiba Scientific, Kyoto, Japan), and termed X-RAW, in which X is the initial of the botanic specie (B: Brachypodium; F: flax; H: hemp; J: jute; S: sisal; N: nettle).

Prior to the analysis, a solvent-extraction step may be necessary to isolate the cell wall material. Soluble compounds were extracted from 200 mg of raw samples with 40 mL of absolute ethanol in a water bath at 60 °C for 1 h before being centrifuged for 10 min at 1459 × g. The liquid phase was removed, and three additional washes were performed similarly. A colorimetric test was performed to verify the absence of free sugars [57,58]. The washed samples were called Alcohol-Insoluble Residues (AIR).

ABSL and CASA methods were performed on batches X-Raw and X-AIR (Table 2) to determine the usefulness of this step on lignin quantification by spectroscopy. We assessed the relative difference

induced by this solvent-extraction step and the possible interference of soluble compounds. The uncertainty arising from this step is calculated by:

EQ 1: Calculation of the uncertainty arising from the Alcohol-Insoluble washing step

$$Minimum\ total\ uncertainty\ on\ the\ final\ value = \frac{\Delta m}{m} + \left(3 \times (\frac{\Delta v}{v} + 0.01) \right) \times 100 = 3.8\%$$

With Δm = uncertainty of the balance (0.1 mg), m = mass weighed (200.0 mg), "3" = number of washing steps, Δv = uncertainty of the volume delivered by the pipette (0.1 mL), v = volume selected (40.0 mL), "0.01" is the fraction – or percentage 1% – of lignin dissolved in absolute ethanol that we set arbitrarily according to the most optimistic scenario for solubilization of the lignin in absolute ethanol, in which only 1% of the lignin was dissolved in this organic solvent. This last value reflects the Hildebrand solubility parameter (δ = 26.5 $MPa^{1/2}$), the Hansen solubility parameter (δ = 15.8 $MPa^{1/2}$) of absolute ethanol, the results of published studies [59,60], and lastly on recommendations from the thesis of Bouxin [61].

2. Klason lignin (KL) content

Total KL determination has been performed following the "Acid-insoluble lignin in wood and pulp" TAPPI 222 om-02 normalized method with slight modifications [62,63]. Ground powder (300 mg) of the X-Raw sample was hydrolyzed by 5 mL of 72% sulfuric acid solution for 1 h at room temperature under agitation with glass beads. The sample was then diluted with 193.5 g of ultrapure water to reduce the sulfuric acid concentration to 3% prior to autoclaving for 1 h at 120 °C. After cooling, the hydrolysate was filtered through a 48 mm sintered glass funnel filter with porosity 3. The residue is washed twice using 800 mL ultrapure water to achieve a neutral pH. The funnel with acid-insoluble residue was dried at 105 °C for 16 h and then cooled in a desiccator. The dried insoluble residue, representing the KL content, was determined by weighing. Each sample was assayed in duplicate.

3. Acetyl Bromide Soluble Lignin method (ABSL)

An adaptation of the ABSL method [42] was utilized wherein 7 mg of each sample were dissolved in 1.5 mL of glacial acetic acid (HOAc) and 0.5 mL of AcBr. The mixture was heated for 2 h and 30 min at 55 °C with a stirring of 500 rpm using an MB-102 thermomixer (Bioer, Potsdam, Germany). After cooling to room temperature for 10 min, 200 µL of the sample was added to 3 mL of a NaOH/HOAc solution (250 mL glacial HOAc and 45 mL of 2 M NaOH). Hydroxylamine hydrochloride (500 µL) was quickly added, and the mixture was homogenized. The absorbance was measured at 280 nm after precisely 1 h using a UV 3100 PC spectrophotometer (VWR, Radnor, Pennsylvania, USA). Based on Beer-Lambert's law, the lignin content was calculated from:

EQ 2: Beer-Lambert's Law applied to the AcBr method

$$C = \frac{A}{\varepsilon . l}$$

With A = Absorbance measured at 280 nm, ε = extinction coefficient (20 $L.g^{-1}.cm^{-1}$), l = length of the light path = 1 cm, and C = lignin content ($g.L^{-1}$)

4. Cysteine-Assisted Sulfuric Acid method (CASA)

The method presented in [49] was adapted to measure the lignin content. Approximately 10 (±0.1) mg of previously ground powder of X-Raw samples were weighed for the experiment. The powder was dissolved in 1 mL of a mixture at 1 g/L L-cysteine in 72% sulfuric acid for 1 h, at 24 °C with a stirring

at 500 rpm using an MB-102 thermomixer (Bioer, Potsdam, Germany). Samples were diluted 10× with distilled water before absorbance measurement and diluted 10× if the absorbance was greater than 1.000 u.a. (resulting in a total dilution factor of 100, as has been used for Brachypodium and jute). Absorbance was measured at 283 nm with a UV 3100 PC spectrophotometer (VWR, Radnor, Pennsylvania, USA). The same process was applied to samples X-AIR in order to measure the effect of the washing step on the result. The total lignin content was calculated with the EQ 2, with an absorption coefficient based on the results of the KL and the ABSL techniques.

5. Thioacidolysis for the aromatic lignin unit distribution

This method is adapted from [64] and [65]. Briefly, 10 mg of alcohol-insoluble cell wall residue (AIR) were incubated in 3 mL of dioxane with ethanethiol (10%) and BF_3-etherate (2.5%) and 0.1 mL of internal standard solution (heneicosane C21, 2.5 mg/mL, diluted in CH_2Cl_2) at 100 °C for 4 h. $NaHCO_3$ (0.2 M, 3 mL) was added after cooling and mixed before adding 0.1 mL of HCl (6 M). The tubes were vortexed after adding 3 mL of dichloromethane, and the lower organic phase was collected in a new tube before concentration under a nitrogen atmosphere to approximately 0.5 mL. A 10 µL aliquot was then trimethylsilylated (TMS) with 100 µL of *N,O*-bis(trimethylsilyl) trifluoroacetamide, and 10 µL of ACS-grade pyridine. Aliquots (1 µL) of the trimethylsilylated samples were injected into an Agilent 5973 Gas Chromatography-Mass Spectrometry system. Selected-ion chromatograms reconstructed at m/z 239, 269, and 299 were used to quantify H, G, and S lignin monomers, respectively, and compared to the internal standard at m/z 57, 71, 85.

6. Calculation of the Pearson Correlation Coefficient (PCC)

The PCC (Fig. 2) examines the relationship between two variables and determines the influence of one on the other. This coefficient varies from -1 to +1 and corresponds to the "r" of the linear regression curve f(x)=y, where x and y are the two variables. If the PCC is equal to -1 or +1, there is a strong correlation between the two sets of data; conversely, if the PCC is close to 0, there is no correlation.

EQ 3: Pearson's correlation coefficient equation

$$r = \frac{n\sum xy - (\sum x \sum y)}{\sqrt{n\sum x^2 - (\sum x)^2}\sqrt{n\sum y^2 - (\sum y)^2}}$$

Where n = number of values x and y

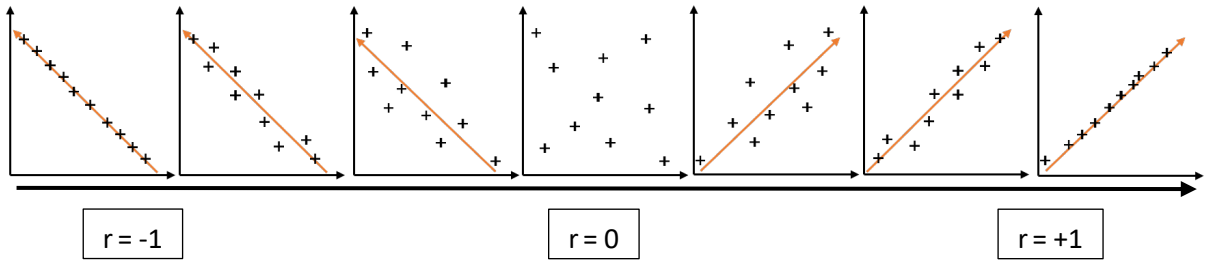

Fig. 2. Graphical representation of the Pearson Correlation.

Results and discussion

1. Alcohol-Insoluble Residue (AIR): Necessity of the washing step

For KL, ABSL, and CASA methods, the determination has historically been carried out on the isolated cell wall material, commonly termed the Alcohol-Insoluble Residue (AIR). The solvent extraction step is necessary before performing the lignin quantification to remove cellular metabolism artifacts and some polyphenols not attached to the fiber cell wall that can lead to an overestimation of the total lignin content in the sample [66]. Because some researchers choose to circumvent this step, we examined the ramifications of not extracting and using the whole biomass versus using the AIR.

The necessity of this step was assessed by comparing the relative differences between the results obtained on pre-extracted samples (X-AIR) vs. unextracted biomass (X-RAW) (Fig. 3). Fiber bundles from fibrous plants do not contain high levels of soluble compounds compared to other plant biomass. Lignin content consequently varies only slightly between non-extracted and extracted samples, regardless of the technique. We calculated a mean relative difference of 0.91% with specific values ranging from 0.3% for sisal to 2.1% for flax when the ABSL method was used. When CASA was used, the mean relative difference was slightly higher (1.24%), with values ranging from 0.37% for hemp to 2.7% for jute; the difference was 0.42% for jute and less than 0.1% for all the other annual fibrous plants, including flax.

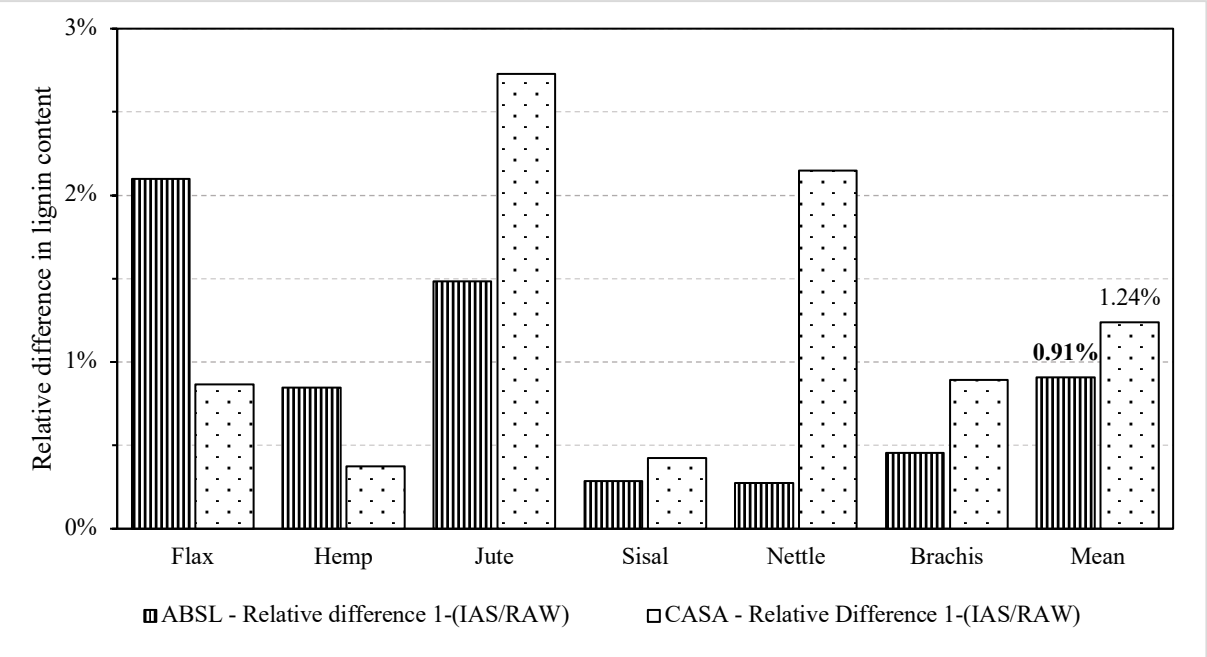

Fig 3. Relative difference in lignin content (%) between samples according to an Insoluble-Alcohol Residues washing step or not, using the "Acetyl Bromide Soluble Lignin" and the "Cysteine-Assisted Sulfuric Assisted" methods.

The impact of solvent-extracting the stem on lignin quantification for annual plant fibers was therefore determined to be very low. According to EQ1, it even causes more inaccuracy (at least 3.8% relative difference) than with the improvements in estimating the lignin content for these materials.

2. Determination of the UV absorption coefficient ε and its relationship to aromatic lignin unit ratio G:S:H

We obtained contrasting results between the KL and the ABSL methods (Fig. 4). The KL method is a gravimetric method, the ABSL is spectrophotometric, and a mean relative difference of 15% has already been determined [41]. For flax, the KL method led to higher values than ABSL, whereas we obtained the opposite for sisal and Brachypodium, with an overestimation of lignin by the ABSL method

compared to Klason. For hemp, jute, and nettle, lignin contents were almost equivalent between all methods, and there was no significant difference using a T-Test (95% confidence level).

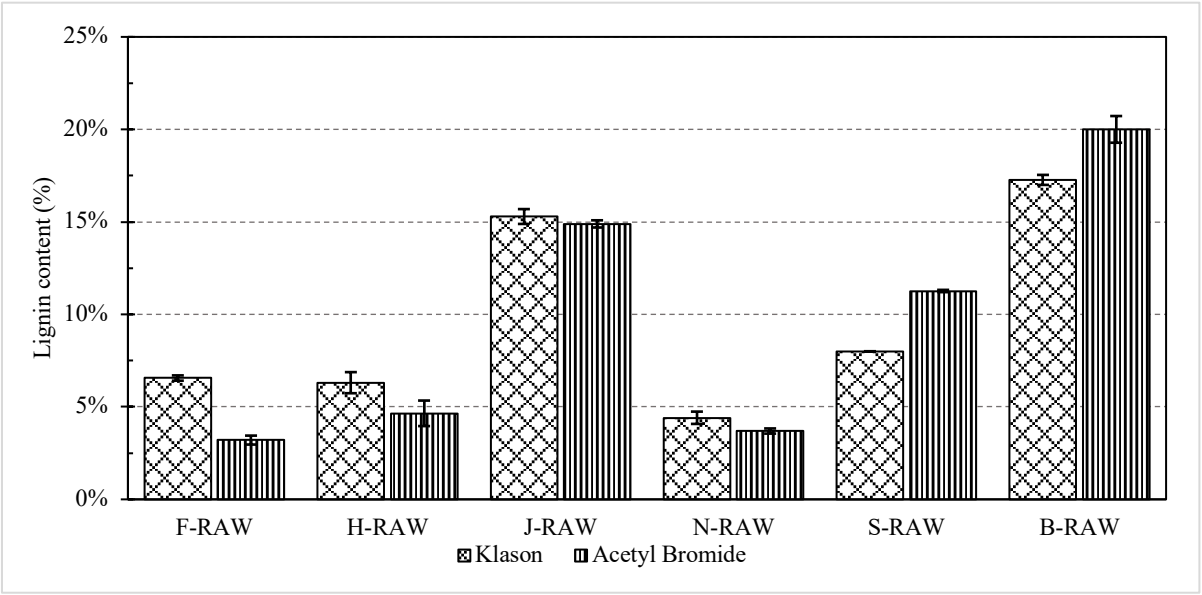

Fig. 4. Lignin content (%) measured by KL and ABSL methods on different botanical species.

Lignin structure and composition may impact the dissolution under acidic conditions. Indeed, the monomers are bonded by different inter-unit linkages, requiring distinctly different energies to break and/or solubilize. Each type of aromatic unit has a slightly different molar absorption coefficient at a given wavelength. To determine the most appropriate absorption coefficient, a CASA experiment on the X-Raw samples was performed using six replicates. Then, the CASA ε was calculated based on KL or ABSL contents (Table 3).

Sample	%G	%S	%H	S/G	H/S	H/G	ε (L .g-1.cm-1)	
							calculated based on ABSL method	calculated based on KL method
Flax	93%	2%	5%	0.02	2.22	0.05	22.6	11.0
Nettle	65%	35%	1%	0.53	0.02	0.01	17.4	14.5
Hemp	62%	38%	0%	0.61	0.00	0.00	15.5	11.4
Jute	26%	73%	0%	2.77	0.01	0.01	11.8	11.3
Brachypodium	29%	67%	5%	2.31	0.07	0.16	11.4	13.2
Sisal	25%	75%	0%	3.02	0.00	0.00	7.1	10.0
PCC ε based on ABSL method (r^2)	0.96	-0.96	0.46	-0.93	0.75	-0.04	1.00	0.26
PCC ε based on KL method (r^2)	0.12	-0.13	0.15	-0.31	-0.25	0.33	0.26	1.00

Table 3. Monomer content, ratios, calculated molar absorption coefficients, and Pearson correlations for each annual plant.

The outcomes established a range of ε from 7.14 $L.g^{-1}.cm^{-1}$ (sisal) to 22.68 $L.g^{-1}.cm^{-1}$ (flax). We linked these values to the lignin unit ratio determined from the distribution of monomers used in lignification in the samples. Monomer composition was assessed by thioacidolysis (Table 3), and from

the %G, %S, and %H values, we determined the ratio S/G, H/S, and H/G ratios. Thioacidolysis degrades lignin by cleaving β-O-4 bonds. Only the non-condensed units are therefore analyzed, and the monomer distribution represents only a fraction of the total lignin [64,65,67]. The results obtained (Table 3) reflect various distributions in the ratio of the monomers G:S:H among the different phylogenetic species; samples having mainly G-lignin included hemp (93%), flax (93%), and nettle (69%), whereas jute and sisal had primarily S-lignin (73% and 83%, respectively). H-lignin is always minor, with a ratio varying from <1% (jute, sisal, and nettle) to 6% in hemp. We surmised that the molar absorption coefficient ε relied on the aromatic unit distribution. It can, therefore, fit into a full equation, including the absorption contributed by each monomer:

EQ 4: Relation between molar absorption coefficient and monolignol ratio, derived from EQ 2 :

For lignin content, with l . C = %Lignin in the sample

$$A = \varepsilon \,.\, \%\text{Lignin}$$

Via the CASA method, lignin may be cleaved into small pieces. The overall absorbance is contributed from the three types of aromatic units derived from the three monolignols, with various efficiencies

$$A^{283nm} = \left(\varepsilon^{283nm}_{G-Lignin} \,.\, \text{G}\right) + \left(\varepsilon^{283nm}_{S-Lignin} \,.\, \text{S}\right) + \left(\varepsilon^{283nm}_{H-Lignin} \,.\, \text{H}\right)$$

By replacing the various espilons by x, y, and z to simplify the equation, and adding interaction coefficients, we can write the following:

$$A^{283nm} = \varepsilon^{283nm}_{Monolignols} \times \%\text{Lignin}$$

$$\varepsilon^{283nm}_{Monolignols} = [\boldsymbol{x} \times (\boldsymbol{G}) + \boldsymbol{y} \times (\boldsymbol{S}) + \boldsymbol{z} \times (\boldsymbol{H})] + [\boldsymbol{u} \times (\boldsymbol{S/G}) + \boldsymbol{v} \times (\boldsymbol{H/S}) + \boldsymbol{w} \times (\boldsymbol{H/G})]$$

With:

- $\varepsilon^{283nm}_{Monolignols}$ = total molar absorption coefficient ($L.g^{-1}.cm^{-1}$);
- G, S, and H = proportion of G-Lignin, S-Lignin, and H-Lignin (in %);
- G + H + S = 1;
- x, y, and z = molar absorption coefficients (respectively from G-lignin, S-lignin, and H-lignin) ($L.mol^{-1}.cm^{-1}$);
- u, v, and w = overlapping coefficients between two absorbance peaks (respectively S/G, H/S, and H/G).

The Pearson Correlation Coefficient (PCC) was calculated (EQ3) to verify that monomer percentage and ratios were relevant (Table 3). For calculations based on ABSL results, the G-lignin ratio, S-lignin ratio, and S/G are the most pertinent factors for calculating ε, with an R^2 above 0.90. The H/S ratio also seemed to have an influence ($R^2 = 0.75$). However, based on KL results, no factor was decisive for the calculation of the applicable ε. Indeed, each absolute value of PCC was lower than 0.35, meaning there was no correlation between the ε based on Klason results and the monomer ratio. Finally, there was a low correlation between the KL or ABSL related to the calculated ε ($R^2 = 0.26$), meaning that there was a significant difference when using one of the other methods.

3. Verification of the accuracy of the previously determined ε and optimization of this coefficient on five hemp industrial varieties

As described in the previous paragraph, we determined two absorption coefficients for hemp: one calculated from the results of Klason ($\varepsilon_{hemp,KL}$ = 11.47 $L.g^{-1}.cm^{-}1$) and one from ABSL ($\varepsilon_{hemp,ABSL}$ = 15.55 $L.mol^{-1}.cm^{-1}$). In order to determine which absorption coefficient is the most accurate compared to the

KL reference method, we calculated the relative difference (%) with the EQ4 between KL and CASA on five industrial hemp varieties (Fig. 5).

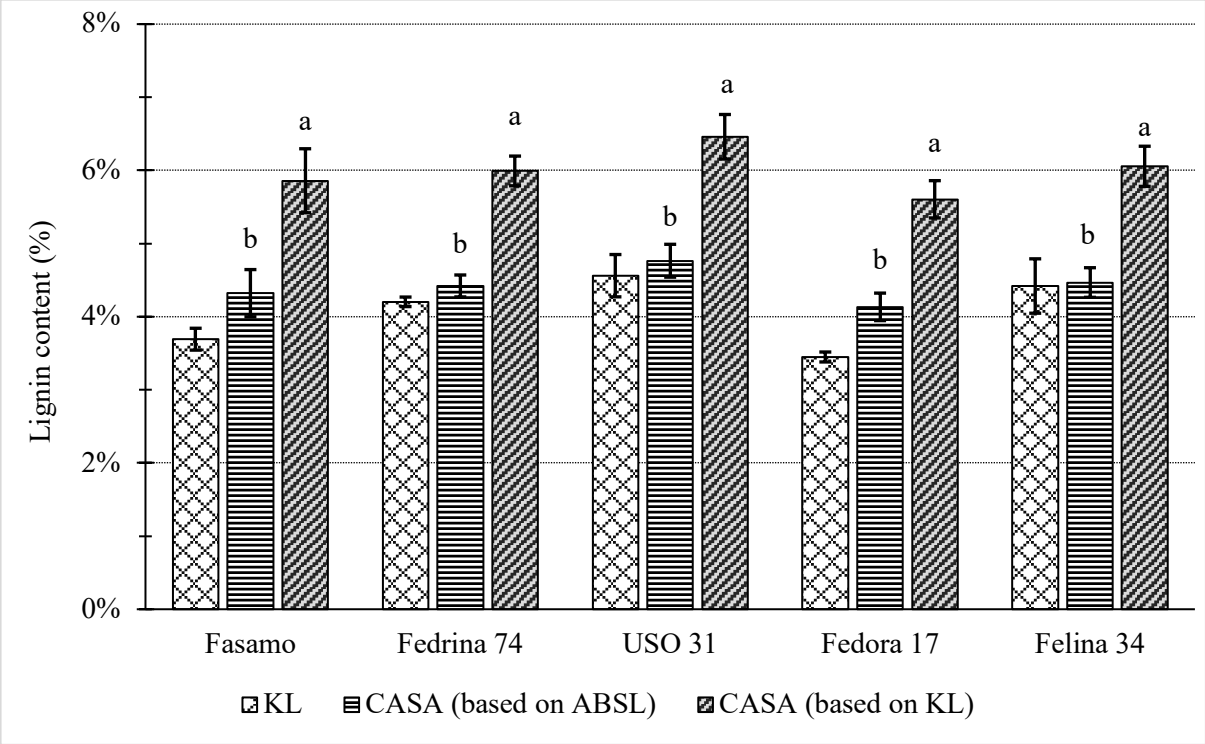

Fig. 5. Comparison of lignin content in industrial hemp varieties obtained by KL and CASA methods, with Epsilon calculated based on KL and ASBL content of annual plant fibers. (a) significative difference (T-Test 95% with Klason). (b) no significative difference (T-Test 95% with Klason).

EQ 5: Calculation of the relative difference (%) between results obtain with Klason and CASA

$$\text{Relative difference (\%)} = 1 - \frac{\text{Lignin content obtained with CASA method}}{\text{Lignin content obtained with Klason reference method}}$$

Utilizing $\varepsilon_{hemp,ABSL}$ lead to a lower relative difference between CASA and Klason for the industrial hemp varieties than the results obtained via $\varepsilon_{hemp,KL}$ of 11.47 $L.mol^{-1}.cm^{-1}$. Specifically, with the calculated $\varepsilon_{hemp,ABSL}$ of 15.55 $L \cdot mol^{-1} \cdot cm^{-1}$, three out of five industrial hemp species exhibited a relative difference of less than 5% when compared to KL (Table 4), as calculated using EQ4. Only Fedora 17 demonstrated a relative difference exceeding 15%, specifically 16.5%, which represents a significant difference between KL and ABSL for the same variety mentioned in the literature [41]. Using $\varepsilon_{hemp,KL}$ of 11.47 $L.mol^{-1}.cm^{-1}$ led to an overestimation of the lignin content in every industrial hemp with the CASA method. None of the results are in the confidence zone with a Student's T-Test with a 95% degree (Fig. 5). This significant difference can likely be attributed to the distinct methodologies employed in each technique to determine $\varepsilon_{hemp,ABSL}$ and $\varepsilon_{hemp,KL}$. KL utilizes a thermogravimetric approach. Lignin is condensed during the process and depends less on the chemical structure of lignins, so the result itself is not impacted by the monomeric distribution. On the other hand, ABSL solubilizes the whole wall material and, in principle, measures all aromatics by spectrophotometry, as does CASA. These two methods also exhibit the same high sensitivity to the structural variations in aromatic lignin unit distributions, as well as to the precise chemical composition of the samples. Small chemical structural changes involving phenolic groups can induce notable shifts in the absorbance spectra, impacting the measurement of lignin content. Unsaturated side-chains associated with phenolic structures can further influence the optimal wavelength for aromatic absorption, thereby affecting the accuracy of the results

[49]. From these results, the $\varepsilon_{hemp,ABSL}$ of 15.55 $L \cdot mol^{-1} \cdot cm^{-1}$, has been selected as the most suitable molar absorption coefficient (ε) for lignin analysis of hemp fibers with the CASA method.

There are slight variations in the accuracy of CASA depending on the hemp variety. To elucidate the relative differences observed (Fig 5.), thioacidolysis was conducted on the same hemp cultivars. The results are presented in Table 4 and are compared to the hemp H-Raw sample, which have been utilized to determine the extinction coefficient $\varepsilon_{hemp,ABSL}$ of 15.55 $L.mol^{-1}.cm^{-1}$. The absolute value of the relative difference in the syringyl-to-guaiacyl (S/G) ratio between industrial hemp and H-Raw aligns with the relative difference in lignin content as measured by KL and CASA (Fig. 6). Specifically, H-Raw exhibited a lower S/G ratio of 0.608, in contrast to the industrial hemp varieties that had an average S/G ratio of 0.745 ± 0.036.

		With : ε = 15.55 $L.g^{-1}.cm^{-1}$		G	S	H	S/G
		Absolute difference	Relative difference				
Hemp H-Raw		0% : used to determine the ε		62.1%	37.7%	0.17%	0.60
Industrial hemp varieties	Fasamo	0.63%	14.5%	55.3%	44.7%	0%	0.80
	Fedrina 74	0.22%	4.91%	58.1%	41.9%	0%	0.72
	USO 31	0.20%	4.29%	58.5%	41.5%	0%	0.70
	Fedora 17	0.69%	16.5%	53.0%	47.0%	0%	0.88
	Felina 34	0.05%	1.07%	62.4%	37.6%	0%	0.60
Mean Industrial Hemp Varieties		0.36 % (±0.28)	8.28 % (±6.86)	57.5 % (±3.6)	42.5 % (±3.6)	0 %	0.74 (±0.03)

Table 4. Relative difference (%) of lignin content in industrial hemp varieties measured by KL and CASA using the previously determined ε = 15.55 $L.g^{-1}.cm^{-1}$, and the relative composition of monomers released by thioacidolysis.

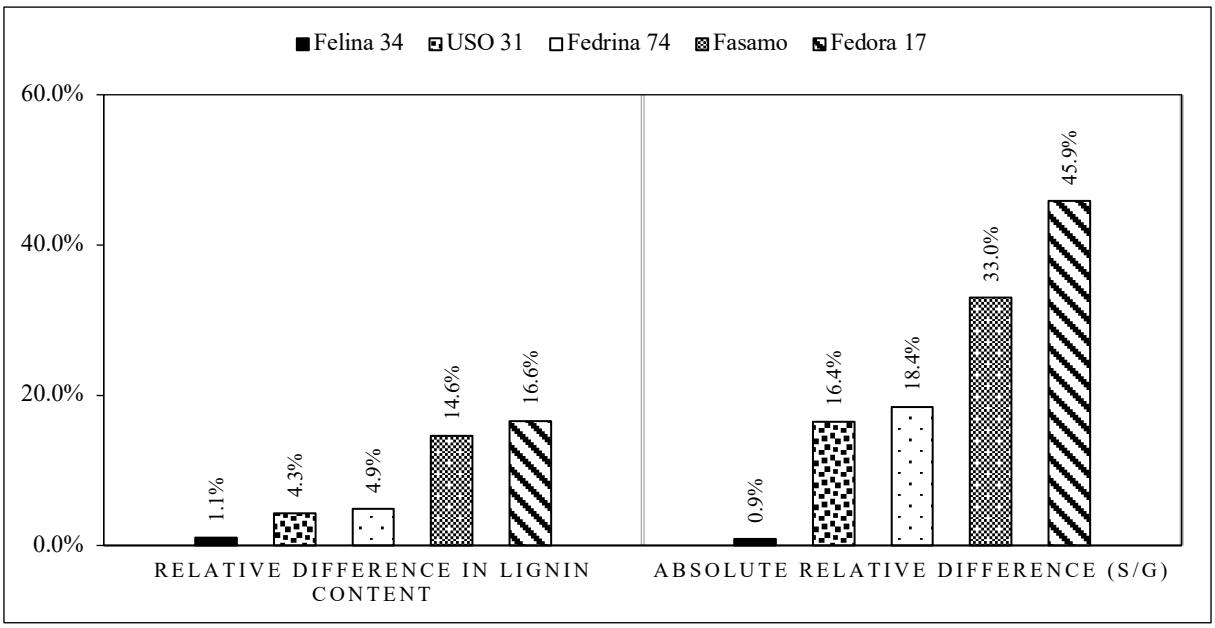

Fig. 6. Relative difference in lignin content between KL and CASA methods, and in S/G, between H-Raw and the five industrial hemp varieties.

Thioacidolysis has elucidated the relationship between the absorption molar coefficient (ε) and the ratio of aromatic lignin units, specifically guaiacyl (G), syringyl (S), and *p*-hydroxyphenyl (H) units. The kinetics of hydrolysis are influenced by the lignin composition. Monolignols are interconnected through various chemical bonds, with the β-O-4 ether bond being particularly significant in the dissolution kinetics [68]. The hemp used for the previous calculation doesn't have a ratio representative of the hemp diversity, leading to a high difference in lignin content between KL and CASA. Further calculation led to an optimized $\varepsilon_{\text{Hemp}}^{283\text{nm}} = 17.03 \pm 1.30\ \text{L.g}^{-1}.\text{cm}^{-1}$ as a mean value. The relative difference varies from +9% to -8% (Fig. 7), with a mean relative difference of zero (0%).

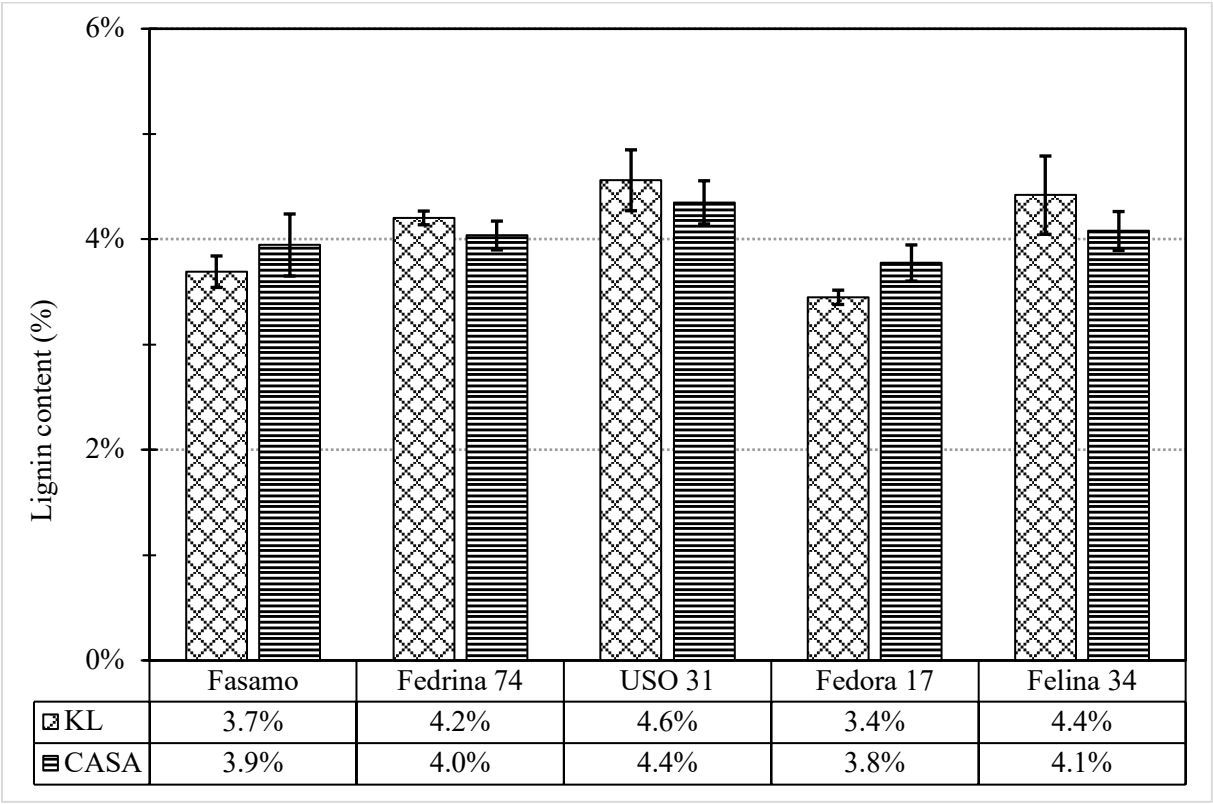

	Fasamo	Fedrina 74	USO 31	Fedora 17	Felina 34
KL	3.7%	4.2%	4.6%	3.4%	4.4%
CASA	3.9%	4.0%	4.4%	3.8%	4.1%

Fig. 7. Lignin content in industrial hemp varieties measured by KL (reference) and CASA, using an ε of 17.03 L.g^{-1}.cm^{-1}

4. Mathematical correlation between ε and the ratios of aromatic lignin units ratio G:S:H

The existence of a correlation between the aromatic unit ratio and the ε has been highlighted in this study. In order to simplify the future use of the CASA method to analyze lignin content in biomass, linear correlations have been plotted (Fig. 8). These allow researchers to quickly estimate the ε to use depending on the monomer content. As shown in Table 3, G-lignin and S-lignin contents are the most relevant factors to estimate ε. S/G is also a suitable candidate for plotting correlation curves with ε. H-lignin contents were too low to accurately conclude anything about their impact on the molar absorption coefficient. $\varepsilon_{Monolignols}^{283nm}$ can be calculated with the equations for the various linear regression (Fig. 8):

$$\text{EQ5}: \quad \varepsilon_{Monolignols}^{283nm} = \frac{(\%\mathbf{G-lignin} + \mathbf{0.2021})}{\mathbf{0.0489}}$$

$$\text{EQ6}: \quad \varepsilon_{Monolignols}^{283nm} = \frac{(\%\mathbf{S-lignin} - \mathbf{1.2119})}{\mathbf{-0.0508}}$$

$$\text{EQ7}: \quad \varepsilon_{Monolignols}^{283nm} = \left(\frac{\%\mathbf{S-lignin}}{\%\boldsymbol{G-lignin}} - \mathbf{4.7514}\right) \div (\mathbf{-0.2234})$$

EQ5 and EQ6 are highly accurate, with an R^2 correlation factor of 0.9150 and 0.9254, whereas using S/G (EQ7) is slightly less so, with an $R^2 = 0.8636$.

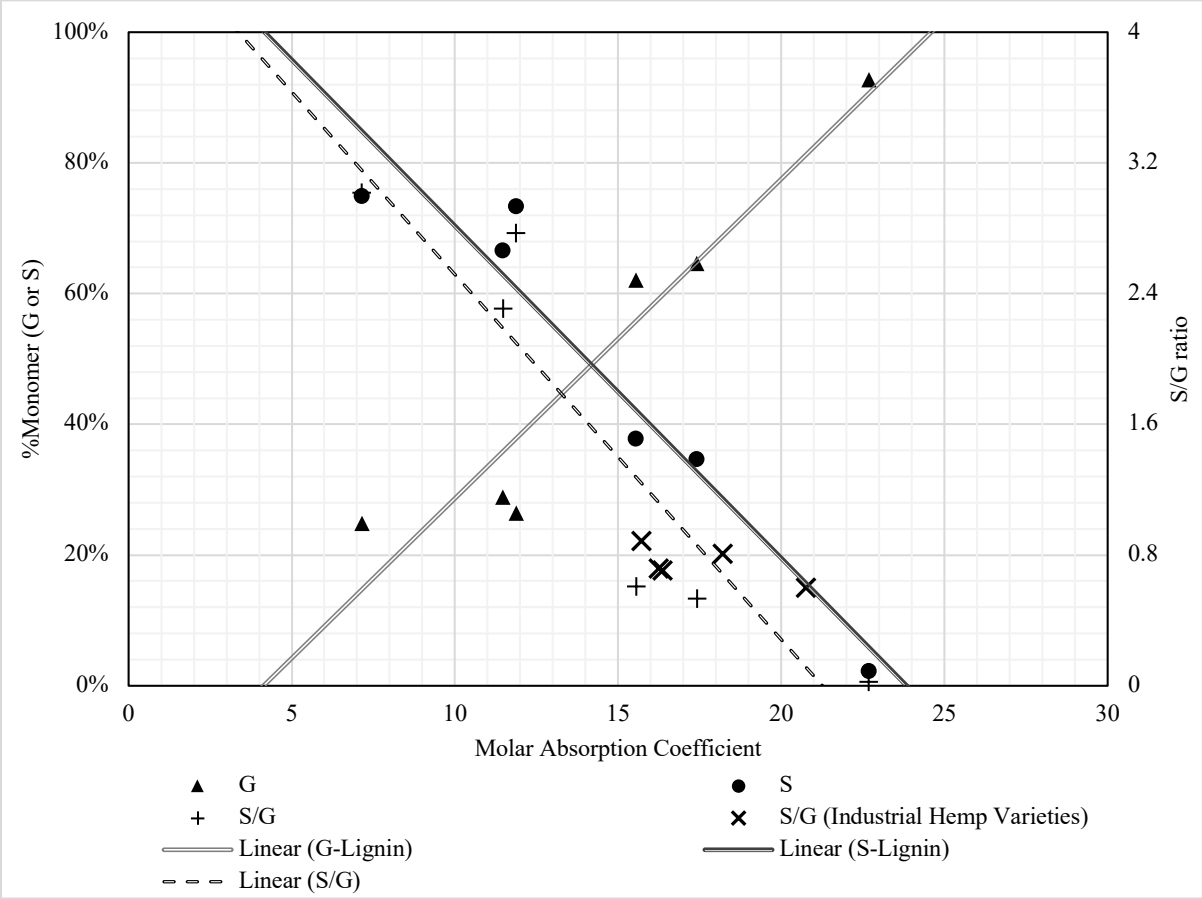

Fig. 8. Abaqus of molar absorption coefficient and different monomer ratios and percentages to determine the most suitable ε to apply to the CASA experiment.

Conclusion

This study demonstrated that the CASA method is a readily applicable technique for measuring lignin content in annual fibrous plants and low-lignin biomass. This method is faster than the Klason reference method and allows for the simultaneous analysis of multiple samples. CASA offers several advantages, including a lower reaction temperature for lignin dissolution and the use of standard reagents instead of carcinogenic, mutagenic, and reprotoxic (CMR) substances. It also requires less sample mass.

However, the CASA method relies on a molar absorption coefficient (ε) that is affected by the monomer ratio of the analyzed sample. In the annual plant fiber bundles studied, ε varied from 7.14 to 22.68 $L \cdot g^{-1} \cdot cm^{-1}$. Compared to the widely used ABSL spectrophotometric method, the results obtained through CASA are more accurate, showing a relative difference of -8% to +9% when compared to the Klason reference across a batch of five industrial hemp varieties. To achieve these results, an optimized ε for hemp was calculated to be 17.03 $L \cdot g^{-1} \cdot cm^{-1}$.

To facilitate the application of these results in other studies, linear correlations have been established to quickly determine the appropriate molar extinction coefficient at 283 nm based on the monomer ratio of the analyzed sample. It is important to note that the guaiacyl:syringyl (G:S) ratios were obtained through thioacidolysis, which quantifies the monomers released after the cleavage of labile linkages. It could be interesting to investigate the monomer ratio with a non-destructive method, such as quantitative

NMR [48,69], before quantifying the lignin content with the CASA method to determine the most suitable ε for the experiment.

Acknowledgment

The authors would like to thank the Phenobois facility for contributing to the Klason Lignin analysis. Phenobois, INRAE, 2018. Wood and Tree Physicochemical Phenotyping Facility for Genetic Resources, https://doi.org/10.15454/1.5572410490640864E12, and the technical staff of INRAE, Sylviane Daniel, Lucie Le Bot and Lèna Brionne, for their support and help during the chemical analysis.

The authors gratefully acknowledge the funding by the ANRT - Association Nationale de la Recherche et de la Technologie, France, under grants 2022/0718. F. Lu and J. Ralph were funded by the DOE Great Lakes Bioenergy Research Center (DOE BER Office of Science DE-SC0018409).

References

1. Cell Wall, in Esau's Plant Anatomy. 2006. p. 65-101.
2. Structure and development of the plant body—an overview, in Esau's Plant Anatomy. 2006. p. 1-13.
3. Komuraiah, A., N.S. Kumar, and B.D. Prasad, Chemical composition of natural fibers and its influence on their mechanical properties. Mechanics of Composite Materials, 2014. **50**(3): p. 359-376. https://doi.org/10.1007/s11029-014-9422-2
4. Chokshi, S., et al., Chemical composition and mechanical properties of natural fibers. Journal of Natural Fibers, 2022. **19**(10): p. 3942-3953. https://doi.org/10.1080/15440478.2020.1848738
5. Madsen, B., T.L. Andersen, and H. Lilholt, Volumetric composition: fiber content and porosity, in Handbook of Green Materials, Vol 4: Biobased Composite Materials, their Processing Properties and Industrial Applications, K. Oksman, et al., Editors. 2014. p. 137-153.
6. Gibson, L.J., The hierarchical structure and mechanics of plant materials. Journal of the Royal Society Interface, 2012. **9**(76): p. 2749-2766. https://doi.org/10.1098/rsif.2012.0341
7. Erdtman, H., Lignins: occurrence, formation, structure and reactions. Journal of Polymer Science Part B: Polymer Letters, 1972. **10**(3): p. 228-230. https://doi.org/10.1002/pol.1972.110100315
8. Wu, G., M. Heitz, and E. Chornet, The depolymerization of lignin via aqueous alkaline oxidation, in Advances in Thermochemical Biomass Conversion, A.V. Bridgwater, Editor. 1993, Springer Netherlands: Dordrecht. p. 1558-1571.
9. Blandinières, H. and S. Amaducci, Adapting the cultivation of industrial hemp (*Cannabis sativa L.*) to marginal lands: A review. Global Change Biology Bioenergy, 2022. **14**(9): p. 1004-1022. https://doi.org/10.1111/gcbb.12979
10. Burton, R.A., et al., Industrial hemp seed: from the field to value-added food ingredients. Journal of Cannabis Research, 2022. **4**(1): p. 45. https://doig.org/10.1186/s42238-022-00156-7
11. Lopez, C., et al., Deciphering the properties of hemp seed oil bodies for food applications: lipid composition, microstructure, surface properties and physical stability. Food Research International, 2021. **150**. https://doi.org/10.1016/j.foodres.2021.110759
12. Beaugrand, J., et al., Multi-scale analysis of the structure and mechanical performance of woody hemp core and the dependence on the sampling location. Industrial Crops and Products, 2014. **60**: p. 193-204. https://doi.org/10.1016/j.indcrop.2014.06.019
13. Yang, Y., et al. Study on development of hemp stem-based panel. in *4th International Conference on Advances in Materials and Manufacturing (ICAMMP 2013)*. 2013.
14. Arango, S., et al., Physical characterization of ten hemp varieties to use as animal bedding material. Animals, 2023. **13**(2): p. 284. https://doi.org/10.3390/ani13020284

15. Manian, A.P., M. Cordin, and T. Pham, Extraction of cellulose fibers from flax and hemp: a review. Cellulose, 2021. **28**(13): p. 8275-8294. https://doi.org/10.1007/s10570-021-04051-x
16. Bourmaud, A., et al., Main criteria of sustainable natural fibre for efficient unidirectional biocomposites. Composites Part A: Applied Science and Manufacturing, 2019. **124**. https://doi.org/10.1016/j.compositesa.2019.105504
17. Petit, J., et al., Phenotypic variation of cell wall composition and stem morphology in hemp (*Cannabis sativa L.*): optimization of methods. Frontiers in Plant Science, 2019. **10**: p. 959. https://doi.org/10.3389/fpls.2019.00959
18. Snegireva, A., et al., Intrusive growth of primary and secondary phloem fibres in hemp stem determines fibre-bundle formation and structure. AoB Plants, 2015. **7**: p. plv061. https://doi.org/10.1093/aobpla/plv061
19. Bourmaud, A., et al., Exploring the mechanical performance and in-planta architecture of secondary hemp fibres. Industrial Crops and Products, 2017. **108**: p. 1-5. https://doi.org/10.1016/j.indcrop.2017.06.010
20. Gautreau, M., et al., Impact of cell wall non-cellulosic and cellulosic polymers on the mechanical properties of flax fibre bundles. Carbohydrate Polymers, 2022. **291**: p. 119599. https://doi.org/10.1016/j.carbpol.2022.119599
21. Fuentes, C.A., et al., Effect of the middle lamella biochemical composition on the non-linear behaviour of technical fibres of hemp under tensile loading using strain mapping. Composites Part A: Applied Science and Manufacturing, 2017. **101**: p. 529-542. https://doi.org/10.1016/j.compositesa.2017.07.017
22. Sanyal, T., Jute, jute fiber, and jute yarn, in Jute Geotextiles and Their Applications in Civil Engineering. 2017. p. 7-17.
23. Viotti, C., et al., Nettle, a long-known fiber plant with new perspectives. Materials, 2022. **15**(12): p. 4288.
24. Veerasimman, A., et al., Thermal properties of natural fiber sisal based hybrid composites – A brief review. Journal of Natural Fibers, 2022. **19**(12): p. 4696-4706. https://doi.org/10.1080/15440478.2020.1870619
25. Boopalan, M., M.J. Umapathy, and P. Jenyfer, A comparative study on the mechanical properties of Jute and Sisal fiber reinforced polymer composites. Silicon, 2012. **4**(3): p. 145-149. https://doi.org/10.1007/s12633-012-9110-6
26. Mishra, R., et al., Bio-composites reinforced with natural fibers: comparative analysis of thermal, static and dynamic-mechanical properties. Fibers and Polymers, 2020. **21**(3): p. 619-627. https://doi.org/10.1007/s12221-020-9804-0
27. Feng, P., et al., Novel lignin-functionalized waterborne epoxy composite coatings with excellent anti-aging, UV resistance, and interfacial anti-corrosion performance. Small, 2024. **20**(28): p. e2312085. https://doi.org/10.1002/smll.202312085
28. Kuperman, A.M., et al., Physical-mechanical properties of fibers made from scoria and materials based on them. Glass and Ceramics, 2009. **66**(7-8): p. 245-248. https://doi.org/10.1007/s10717-009-9174-y
29. Cerchiara, T., et al., Chemical composition, morphology and tensile properties of spanish broom (*Spartium junceum L.*) fibres in comparison with flax (*Linum usitatissimum L.*). Fibres & Textiles in Eastern Europe, 2014. **22**(2): p. 25-28.
30. Nuez, L., et al., Determinant morphological features of flax plant products and their contribution in injection moulded composite reinforcement. Composites Part C: Open Access, 2020. **3**: p. 100054. https://doi.org/10.1016/j.jcomc.2020.100054
31. Moriana, R., et al., Correlation of chemical, structural and thermal properties of natural fibres for their sustainable exploitation. Carbohydrate Polymers, 2014. **112**: p. 422-431. https://doi.org/10.1016/j.carbpol.2014.06.009
32. Mayer-Laigle, C., et al., Unravelling the consequences of ultra-fine milling on physical and chemical characteristics of flax fibres. Powder Technology, 2020. **360**: p. 129-140. https://doi.org/10.1016/j.powtec.2019.10.024

33. Guillou, E., et al., In-situ monitoring of changes in ultrastructure and mechanical properties of flax cell walls during controlled heat treatment. Carbohydrate Polymers, 2023. **321**: p. 121253. https://doi.org/10.1016/j.carbpol.2023.121253
34. Lu, C., et al., Structural and mechanical properties of hemp fibers: effect of progressive removal of hemicellulose and lignin. Journal of Natural Fibers, 2022. **19**(16): p. 13985-13994. https://doi.org/10.1080/15440478.2022.2113851
35. Spies, P.-A., et al., Cellulose lattice strains and stress transfer in native and delignified wood. Carbohydrate Polymers, 2022. **296**: p. 119922. https://doi.org/10.1016/j.carbpol.2022.119922
36. Padovani, J., et al., Beating of hemp bast fibres: an examination of a hydro-mechanical treatment on chemical, structural, and nanomechanical property evolutions. Cellulose, 2019. **26**(9): p. 5665-5683. https://doi.org/10.1007/s10570-019-02456-3
37. Musio, S., J. Müssig, and S. Amaducci, Optimizing hemp fiber production for high performance composite applications. Frontiers in Plant Science, 2018. **9**. https://doi.org/10.3389/fpls.2018.01702
38. Grégoire, M., et al., Comparing flax and hemp fibres yield and mechanical properties after scutching/hackling processing. Industrial Crops and Products, 2021. **172**: p. 114045. https://doi.org/10.1016/j.indcrop.2021.114045
39. Hatfield, R.D., et al., A comparison of the insoluble residues produced by the Klason lignin and acid detergent lignin procedures. Journal of the Science of Food and Agriculture, 1994. **65**(1): p. 51-58. https://10.1002/jsfa.2740650109
40. Sluiter, A., et al., Determination of structural carbohydrates and lignin in biomass in laboratory analytical procedure (LAP). National Renewable Energy Laboratory, 2008.
41. Moreira-Vilar, F.C., et al., The acetyl bromide method is faster, simpler and presents best recovery of lignin in different herbaceous tissues than Klason and thioglycolic acid methods. PLoS One, 2014. **9**(10): p. e110000. https://doi.org/10.1371/journal.pone.0110000
42. Fukushima, R.S. and R.D. Hatfield, Extraction and isolation of lignin for utilization as a standard to determine lignin concentration using the acetyl bromide spectrophotometric method. Journal of Agricultural and Food Chemistry, 2001. **49**(7): p. 3133-3139. https://doi.org/10.1021/jf010449r
43. Soest, P.J.V. and R.H. Wine, Use of detergents in the analysis of fibrous feeds. IV. Determination of plant cell-wall constituents. Journal of Association of Official Analytical Chemists, 2020. **50**(1): p. 50-55. https://doi.org/10.1093/jaoac/50.1.50
44. Dampanaboina, L., N. Yuan, and V. Mendu, Estimation of plant biomass lignin content using Thioglycolic Acid (TGA). Journal of Visualized Experiments, 2021(173). https://doi.org/10.3791/62055
45. Shimada, N., T. Tsuyama, and I. Kamei, Rapid determination of thioglycolic acid lignin for various biomass samples. Mokuzai Gakkaishi, 2019. **65**(1): p. 25-32. https://doi.org/10.2488/jwrs.65.25
46. Hatfield, R.D., et al., Using the acetyl bromide assay to determine lignin concentrations in herbaceous plants: some cautionary notes. J Agric Food Chem, 1999. **47**(2): p. 628-32. https://doi.org/10.1021/jf9808776
47. Cipriano, D.F., et al., Potential and limitations of ^{13}C CP/MAS NMR spectroscopy to determine the lignin content of lignocellulosic feedstock. Biomass and Bioenergy, 2020. **142**: p. 105792. https://doi.org/10.1016/j.biombioe.2020.105792
48. Bourmaud, C.L., et al., Quantification of native lignin structural features with gel-phase 2D-$HSQC_0$ reveals lignin structural changes during extraction. Angew Chem Int Ed Engl, 2024. **63**(31): p. e202404442. https://doi.org/10.1002/anie.202404442
49. Lu, F., et al., A facile spectroscopic method for measuring lignin content in lignocellulosic biomass. Green Chemistry, 2021. **23**(14): p. 5106-5112. https://doi.org/10.1039/d1gc01507a

50. Raiskila, S., et al., FTIR spectroscopic prediction of mason and acid soluble lignin variation in Norway spruce cutting clones. Silva Fennica, 2007. **41**(2): p. 351-371. https://doi.org/10.14214/sf.301
51. Wang, S.L., et al., Assessment system to characterise and compare different hemp varieties based on a developed lab-scaled decortication system. Industrial Crops and Products, 2018. **117**: p. 159-168. https://doi.org/10.1016/j.indcrop.2018.02.083
52. Bouvier d'Yvoire, M., et al., Disrupting the *cinnamyl alcohol dehydrogenase 1* gene (*BdCAD1*) leads to altered lignification and improved saccharification in *Brachypodium distachyon.* Plant journal for cell and molecular biology, 2013. **73**(3): p. 496-508. https://doi.org/10.1111/tpj.12053
53. Richely, E., et al., Exploring the morphology of flax fibres by X-ray microtomography and the related mechanical response by numerical modelling. Composites Part A: Applied Science and Manufacturing, 2022. **160**: p. 107052. https://doi.org/10.1016/j.compositesa.2022.107052
54. Hamdi, S.E., et al., X-ray computed microtomography and 2D image analysis for morphological characterization of short lignocellulosic fibers raw materials: A benchmark survey. Composites Part A: Applied Science and Manufacturing, 2015. **76**: p. 1-9. https://doi.org/10.1016/j.compositesa.2015.04.019
55. Tanguy, M., Contribution à l'étude de matériaux composites à matrice polypropylène et renforcés par des fibres végétales: de la fibre à la pièce automobile. 2016, Lorient.
56. Richely, E., et al., Measurement of microfibril angle in plant fibres: Comparison between X-ray diffraction, second harmonic generation and transmission ellipsometry microscopies. Composites Part C: Open Access, 2023. **11**: p. 100355. https://doi.org/10.1016/j.jcomc.2023.100355
57. Stevens, B.J.H. and R.R. Selvendran, The isolation and analysis of cell-wall material from the alcohol-insoluble residue of cabbage. Journal of the Science of Food and Agriculture, 1980. **31**(12): p. 1257-1267. https://doi.org/10.1002/jsfa.2740311207
58. Selvendran, R.R., Analysis of cell-wall material from plant-tissues - extraction and purification. Phytochemistry, 1975. **14**(4): p. 1011-1017. https://doi.org/10.1016/0031-9422(75)85178-8
59. Dastpak, A., et al., Solubility study of lignin in industrial organic solvents and investigation of electrochemical properties of spray-coated solutions. Industrial Crops and Products, 2020. **148**: p. 112310 https://doi.org/10.1016/j.indcrop.2020.112310
60. Schuerch, C., The solvent properties of liquids and their relation to the solubility, swelling, isolation and fractionation of lignin. Journal of the American Chemical Society, 1952. **74**(20): p. 5061-5067. https://doi.org/10.1021/ja01140a020
61. Bouxin, F., Solvolyse des lignines: production de synthons aromatiques de faibles masses. 2011.
62. Sluiter, A., et al., Determination of structural carbohydrates and lignin in biomass. Biomass Anal Technol Team Lab Anal Proced, 2004. **2011**: p. 1-14.
63. Sluiter, J.B., et al., Compositional analysis of lignocellulosic feedstocks. 1. Review and description of methods. Journal of Agricultural and Food Chemistry, 2010. **58**(16): p. 9043-53. https://doi.org/10.1021/jf1008023
64. Lapierre, C., B. Pollet, and C. Rolando, New insights into the molecular architecture of hardwood lignins by chemical degradative methods. Research on Chemical Intermediates, 1995. **21**(3-5): p. 397-412. https://doi.org/10.1007/bf03052266
65. Kairouani, A., et al., Cell-type-specific control of secondary cell wall formation by Musashi-type translational regulators in Arabidopsis. Elife, 2023. **12**: p. 88207. https://doi.org/10.7554/eLife.88207
66. Marles, M.A.S., B.E. Coulman, and K.E. Bett, Interference of condensed tannin in lignin analyses of dry bean and forage crops. Journal of Agricultural and Food Chemistry, 2008. **56**(21): p. 9797-9802. https://doi.org/10.1021/jf800888r

67. Lapierre, C. and C. Rolando, Thioacidolyses of pre-methylated lignin samples from pine compression and poplar woods. Holzforschung, 1988. **42**(1): p. 1-4. https://doi.org/10.1515/hfsg.1988.42.1.1
68. Hart, W.E.S., L. Aldous, and J.B. Harper, Nucleophilic cleavage of lignin model compounds under acidic conditions in an ionic liquid: a mechanistic study. ChemPlusChem, 2018. **83**(5): p. 348-353. https://doi.org/10.1002/cplu.201700486
69. Cipriano, D.F., et al., Potential and limitations of ^{13}C CP/MAS NMR spectroscopy to determine the lignin content of lignocellulosic feedstock. Biomass & Bioenergy, 2020. **142**. https://doi.org/10.1016/j.biombioe.2020.105792